Patho-molecular identification of circulating H9N2 avian influenza virus in Egypt

Eman M.S. El Nagar[1], Heba. M. Salem[2*], Maha A.N. Gamal[3], Mohamed A. El-Saied[4]

[1]Veterinary Serum and Vaccine Research Institute (VSVRI), Agriculture Research Center (ARC), Cairo, Egypt.
[2]Department of Poultry Diseases, Faculty of Veterinary Medicine, Cairo University, 12211; Giza, Egypt.
[3]Central Laboratory for Evaluation of Veterinary Biologics (CLEVB), Agriculture Research Center (ARC) Cairo, Egypt.
[4]Department of Pathology, Faculty of Veterinary Medicine, Cairo University, Giza 12211, Egypt.

ARTICLE INFO

ABSTRACT

Avian influenza virus (AIV) poses a serious problem among poultry production sector, low pathogenic avian influenza H9N2 (LPAI H9N2) has been widely spread globally inducing indirect huge economic losses and it considered as a hidden threaten due to its immunosuppressive impact on birds. Therefore, the current work objectives were the molecular detection of the circulating AI H9N2 field strain in Egypt during 2022-2023 with pathogenicity testing of the recovered virus in specific pathogen free (SPF) one day old chicks. Out of 10 suspected tracheal samples that have been collected from different broiler chicken farms in Al Qalyubia governorate only 7 (70%) samples were positive by Reverse transcription Polymerase chain reaction (RT-PCR). The strain that showed a high reproductive ability and high egg infective dose 50 (EID50) (10^9/ µl) on ECE via allantoic sac has been selected for pathogenicity testing in SPF chicks. For pathogenicity testing, 60 SPF chicks were allocated into two groups 30 birds each. G1and G2 were inoculated via oculo-nasal route with 100µl containing 1x 10^6 EID50/ µl virus and 100µl sterile normal saline, respectively. During the experimental time (15 days), no mortalities were recorded in the two groups. The observed clinical signs were mild (ruffled feathers, and depression) in G1, but no clinical signs were observed in G2. During the experiment 3 birds per group were ethically slaughtered to observe the postmortem (PM) and histopathological lesions at 3, 5, 7, 10 and 14 days post-infection (dpi). The observed PM lesions were mild tracheitis, mild pneumonia, subcapsular hemorrhage in liver, enlargement of the spleen, mild atrophy in the pancreas, hemorrhage in the thymus, severe nephritis, and nephrosis with distended ureters with ureates but no macroscopic lesions were detected in the bursa of Fabricius. The virus tropism not restricted only to respiratory, renal, and gastrointestinal tract, but also to the liver, pancreas, and thymus. In conclusion, continuous molecular detection, with pathogenicity testing of circulating AIV is recommended. The authors recommend further full H9 sequence to perform cladogram to the currently tested strain.

Introduction

Avian influenza (AI) viruses contribute a significant hazard to the poultry production sector (Abd El-Hack *et al.*, 2022; Setta *et al.*, 2023). In late 2010, Egypt had exposed to an outbreak of G1-like Low-pathogenic avian influenza (LPAI) H9N2 (El-Zoghby *et al.*, 2012; Monne *et al.*, 2013) since then, LPAIV H9N2 has become prevalent in the Egyptian chicken population, producing significant economic challenges for the poultry industry. AI H9N2 virus isolated form different poultry species including chickens (Wu *et al.*, 2008), pigeons (Nagarajan *et al.*, 2009), turkey, ducks, and geese (Perk *et al.*, 2009) also, it found to be isolated from pigs (Wu *et al.*, 2008). AI H9N2 viruses have been found in a variety of wild bird and domestic poultry species all over the world and have occasionally transmitted to mammalian species such as pigs and humans (Carnaccini and Perez, 2020). The first case of AI H9N2 virus infection in humans was reported in China in 1998 (Peiris *et al.*, 1999) since then, a total of 95 laboratory-confirmed cases of AI H9N2 virus infection in humans have been reported, primarily in China then Egypt, Cambodia, Bangladesh, Pakistan, Oman, India, and Senegal (WHO, 2019; WHO, 2020).

Since AI H9N2 is a low pathogenic virus, it can adapt and spread rapidly through the poultry populations causing immune suppression and vaccination failure especially in case of coinfection with other bacterial and other viral pathogens in poultry farms as well as bad management conditions may exaggerate the severity of the infection (Kishida *et al.*, 2004; Haghighat *et al.*, 2008). Moreover, the possibility of coinfection with the circulating HPAI increases the risk of emerging of newly reasserted strains (Hassan *et al.*, 2020). The AI H9N2 virus causes moderate respiratory infection in the form of coughing, sneezing, rales, and excessive lacrimation, but it can also run asymptomatic courses, particularly in wild avian species (Kye *et al.*, 2021). Other clinical symptoms include a decrease in egg production (14-75%) in breeder or layer flocks, as well as a varied mortality rate (10-60%) in hens (Pusch and Suarez, 2018) also, have been reported and it was enhanced by mixed infection (Rimi *et al.*, 2019). The AI H9N2 virus has gained prominence in recent years because of its involvement in many outbreaks in poultry farms and the macroscopic respiratory lesion is varied and differed (Yehia *et al.*, 2023). Hence the present study aimed to isolation and molecular identification of the circulating H9N2 with excluding to the other most common respiratory co-infections (AI H5N1, Newcastle (ND), infectious bronchitis virus (IBV), & *Mycoplasma*) with experimental pathogenicity testing of the most infective strain in SPF chicks.

Materials and methods

Ethical approval

This work is ethically approved by the Institutional Animal Care and Used Committee (Vet. CU. IACUC) with code Vet CU 03162023705.

Sample collection and sampling area

Samples were collected from 10 different broiler chicken farms lo-

cated in Al Qalyubia governorate suspected of AIV infection with variable mortalities and respiratory signs during 2022-2023. From each farm, 10 freshly dead birds were collected then transferred rapidly on ice box to the lab then birds were examined and showed PM lesions of tracheitis, pneumonia and some cases showed the existence of caseous plug at the trachea bifurcation. Ten tracheal and lung samples were collected per farm, pooled, and kept in a -20°C deep freezer for further investigation.

Virus isolation and propagation on SPF embryonating chicken eggs (ECE)

Pooled tracheal swabs (n=10)/ farm were prepared at hood under complete sterile conditions using sterile isotonic phosphate buffer saline (PBS) pH 7.0 containing antibiotic penicillin (2000 units/ml), streptomycin (2 mg/ml), gentamycin (50 µg/ml) according to OIE (2021). Swabs were centrifuged at cooling centrifuge at 12000 RPM for 2 minutes, the supernatant was filtrated by 0.22 µl syringe filter before use. Nine-day old SPF chicken eggs (n=30); (3 eggs for each swab) were inoculated via the allantoic route with 0.2 ml of the filtrated fluid, sealed with wax and kept at 37°C incubator and examined daily for vitality. Dead eggs chilled at 4°Cand tested for hemagglutination (HA) activity.

Virus identification and titration by Haemagglutination (HA), Haemagglutination inhibition (HI) test

Hemagglutination activity (HA) of the allantoic fluid collected from dead chilled eggs were measured using freshly prepared 1% chicken red blood cells (RBCs), according to OIE (2021). To assess the HI activity of the isolated virus, Haemagglutination inhibition test was performed (OIE, 2021) employing monospecific antisera against H9N2. Mono specific antiserum against other HA viruses (H5N1 and NDV) were used to ensure the purity of virus isolate.

Molecular detection of the isolated virus by Reverse transcription Polymerase chain reaction (RT-PCR)

There were a necessary to identify whether the harvested fluid contain only AIV H9 subtype only or it was contaminated with any other extraneous HA viruses (NDV or H5), also it was of a great concern to detect the cause of the noticed caseous plug in the tracheal bifurcation of the investigated field freshly dead birds and exclude virus diseases suggested to induce them as infectious bronchitis virus (IBV) and bacterial disease (*Mycoplasma*). The primer sets, annealing temperature, and PCR product size used to detect the previously mentioned pathogens were summarized in Table 1.

Nucleic acid extraction and Reverse transcription Polymerase chain reaction (RT-PCR) to the harvested allantoic fluid

Nucleic acid was extracted from the allantoic fluid using (Pure link

RNA Mini Kit, Invitrogen by Thermo Fisher Scientific cat no 12183018A) following the manufacture instruction RNA was extracted and kept at -20°C till use.

Following manufacturer instructions, Quick Guide DiaStar One Step RT-PCR: RT at 50oC for 30 min, one cycle at 95°C for 15 min, then 40 Kit (cat no. DR61-K050DR61-K100) was used using specific primers targeting H5, H9, NDV & IBV (each reaction was done separately). The PCR mixture was prepared, and the cycling conditions were adjusted as follows cycles (95°C for 20 sec, annealing temperature for one min, according to the target primer, primer extension at 72°C for 2 min and a final extension at 72°C for 5 min (1 cycle).

Polymerase chain reaction for identifying the presence of Mycoplasma

Ten pooled lung tissues/ farm were homogenized mechanically using (PRO 200 homogenizer - Pro Scientific USA). Following the manufacture instructions DNA was extracted using GeneJet DNA purification kit (Thermos Scientific cat # K0821). PCR reaction was done according to Kong *et al.* (2001) to identify the presence of *Mycoplasma*.

H9N2 virus titration and Egg Infective Dose 50 (EID50) calculation

From molecularly RT-PCR positive farms, pooled samples were inoculated via allantoic sac route into SPF eggs and the virus was titrated using, tenfold serial dilution in PBS of the virus were inoculated in the allantoic cavity of 10 days embryonated Chicken Eggs (five eggs for each dilution and 0.1 ml for each) and the EID50 was calculated following the standard method of IVPI (2022) and Reed and Munch (1938). The allantoic fluid (AF) showing the highest virus infectivity titer will be selected for pathogenicity testing in the current study.

Experimental pathogenesis of one day old SPF chicks infected with H9N2 virus

One day old SPF chicks obtained from the national project Kom Oshim, Fayoum, Egypt (*n* = 60), (30 chicks/group). Chicks were grown in our lab's bio isolator at veterinary serum and vaccine research institute (VSVRI) on sterile food and water with optimal environmental conditions. Chicks were divided in to two groups; G1: chick received 100µl containing 10^6 EID50/ µl H9N2 virus, G2 inoculated by100µl normal sterile saline through the same route. At 3, 5-, 7-, 10- and 14 dpi, three chicks from each group were humanly scarified and examined for the PM lesions. Thymus, tracheas, lung, liver spleen, kidneys, and bursa, were transferred to 10% freshly prepared formol saline for histopathological examination.

Histopathological examination and scoring system for infected tissue

Samples of trachea, lung, liver, kidney, thymus, pancreas, and intestine were collected from three scarified birds from negative and chal-

Table 1. Primers used for molecular studies.

Target gene	Sequence (5/–3/)	Amplicon size and annealing temp	Reference
H5 gene	F. ACAAAGCTCTATCAAAACCCAAC R. TACCCATACCAACCATCTACCAT	499 bp, 57°C	Chaharaein *et al*. (2009)
H9 gene	F-CTYCACACAGARCACAATGG- R. GTCACACTTGTTGTTGTRTC	488 bp, 55°C	Xie *et al*. (2006)
NDV (*F* gene)	F. GGTGAGTCTATCCGGARGATACAAG R. TCATTGGTTGCRGCAATGCTCT	202 bp, 55°C	Creelan *et al*. (2002)
IBV (*S* gene)	F. CACTGGTAATTTTTCAGATGG R. CTCTATAAACACCCTTACA	464 bp, 55°C	Boroomand *et al*. (2018)
Mycoplasma	MG F AACACCAOAGGCGAAGGCGAG MG R ACGGATTTGCAACTGTTTOTATTGG	530 bp, 58°C	Kiss *et al*. (1997)

lenged groups. Samples were collected at five intervals 3, 5-, 7-, 10- and 14 dpi. Samples were preserved in 10% neutral buffered formalin and processed for routine H&E staining (Bancroft *et al.*, 2013). Slides were examined under a light microscope (Olympus cx33, Japan) linked to Olympus DP27 digital camera with CellSens dimensions software (Olympus, Tokyo, Japan). The lesions' scoring system was assessed as previous research (Mo *et al.*, 1997; Amanollahi *et al.*, 2020). Briefly, the distribution pattern of the inflammatory and necrotic lesions detected in examined tissues was numerically scored as the following: 1 means normal, 2 means focal, 3 means multifocal, and 4 means diffuse lesion. The mean lesion score was calculated for all sampling days within experimental groups. Statistical analysis was performed by graph pad prism using Kruskal-Wallis and Mann-Whitney tests. Data were presented as mean values ± standard deviation (SD) that considered significant differences when $P \leq 0.05$.

Results

Field study

The investigated broiler farms showed variable mortalities ranged from 5- 17% and PM examination of the freshly dead chickens showed different degrees of tracheitis, pneumonia, caseous plug at tracheal bifurcation, severe nephritis and/or nephrosis in the kidney with distended ureters with ureates also, atrophy in bursa and thymus were observed in some cases.

Molecular detection of the isolated virus by Reverse transcription Polymerase chain reaction (RT-PCR)

All the investigated farms were molecularly negative for H5, NDV, IBV and *Mycoplasma*. Out of ten farms only seven farms were molecular positive with 70% detection rate for AI H9N2 virus and showed 488 bp product size targeting the H9 primer (Figure 1).
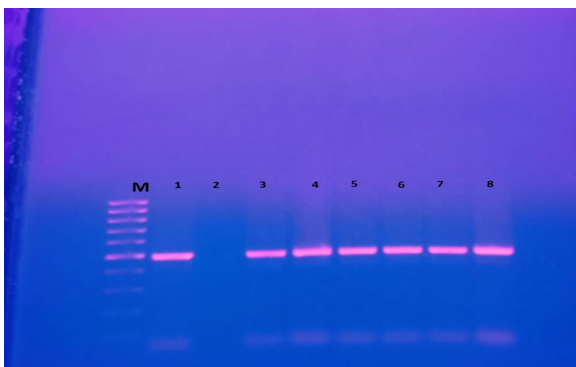
Fig. 1. Photo documentation shows amplification of H9 gene from allantoic fluid inoculated with H9N2 virus, M: is 100 bp gene ruler, Lane 1 control positive, lane 2 control negative, lane 3 to lane 8 showed clear positive band at 488 bp targeting the specific primers.

Virus isolation, propagation on SPF embryonating chicken eggs (ECE), HA and HI tests

During tracheal swabbing of the field samples, the trachea showed hemorrhage and a caseation plug at the tracheal bifurcation. The seven PCR positive pooled swabs subjected to clarification, they were used for SPF egg inoculation according to OIE (2021), the preferred method of growing influenza A viruses is the inoculation of SPF embryonated chicken eggs were inoculated via allantioc sac. Deaths were observed at 48, 51 and 72 hours post inoculation. The infected embryos were hemorrhagic (Figure 2) and the harvested allantoic fluid showed positive slide HA test and HA plate was ranging from 7 to 9 $\log_2$. Allantoic fluid gave positive inhibition titer varies from 5 to 7 $\log_2$ only with anti H9 virus. However, no reaction was observed with the monospecific antisera against other viruses (AI H5, and NDV).
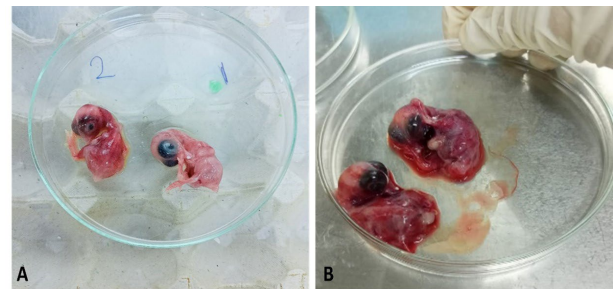
Fig. 2. Representative SPF embryos showed different degrees of hemorrhage due to H9N2 virus infection. A and B embryos died at 48 and 72 hrs. Post inoculation in order.

H9N2 virus titration and Egg Infective Dose 50 (EID50) calculation

According to Reed and Meunch (1938), H9N2 virus titer was ranged from 7 to 9 $\log_{10}$/ µl EID50. The virus that has been selected for pathogenicity testing showed HA plate 29, HI activity 27 and EID50 9 $\log_{10}$.

Experimental pathogenesis of one day old SPF chicks infected with H9N2 virus

During the experimental time (15 days), no mortalities were recorded in the two groups. The observed clinical signs were mild (ruffled feathers, and depression) in G1, but no clinical signs were observed in G2. During the experiment 3 birds per group were ethically slaughtered to observe the PM and histopathological lesions at 3, 5, 7, 10 and 14dpi. The observed PM lesions were mild tracheitis, mild pneumonia, enteritis, subcapsular hemorrhage in liver, enlargement of the spleen, mild atrophy in the pancreas, hemorrhage in the thymus, severe nephritis, and nephrosis with distended ureters with ureates (Figures 3 and 4) but no macroscopic lesions were detected in the bursa of Fabricius.

Table 2. Illustrates the mean of the histological lesion score of different organs at different time points.

Organ	Negative control (Mock)	Lesion score (mean ± SD) Experimentally Infected				
		3 d.	5 d.	7 d.	10 d.	14 d.
Trachea	1.00±0.00 [a]	2.25±0.50 [b]	2.50±0.57 [b]	2.75±0.50 [bc]	3.50±0.57 [bcd]	3.5±0.50 [bcd]
Lung	1.00±0.00 [a]	1.75±0.57 [b]	2.25±0.50 [b]	3.25±0.50 [bc]	3.75±0.50 [bcd]	4.00±0.00 [bcd]
Liver	1.00±0.00 [a]	1.50±0.57 [a]	1.75±0.50 [b]	2.50±0.57 [bc]	3.25±0.50 [bcd]	3.50±0.57 [bcd]
Kidney	1.00±0.00 [a]	1.50±0.57 [a]	2.25±0.50 [bc]	2.50±0.57 [bc]	3.20±0.50 [bcd]	3.50±0.57 [bcd]
Thymus	1.00±0.00 [a]	1.50±0.57 [a]	1.75±0.50 [a]	2.00±0.00 [b]	3.00±0.81 [bc]	3.25±0.95 [bc]
Pancreas	1.00±0.00 [a]	1.50±0.57 [a]	2.00±0.00 [b]	2.50±0.57 [bc]	3.00±0.81 [bcd]	3.00±0.57 [bcd]
Intestine	1.00±0.00 [a]	1.25±0.50 [a]	1.75±0.50 [a]	2.50±0.57 [bc]	3.25±0.95 [bc]	3.75±0.50 [bcd]

[a,b,c,d] Different superscript letters indicate significant differences between values within the same column when $p \leq 0.05$.

Histopathological examination and the lesion score of infected tissues

Figure 5 and Table 2 demonstrated the histopathological alternations of different tissue experimentally infected with LPAI H9 and their lesion score at different time points. Regarding histopathological findings of the tracheal section, the negative control group exhibited normal histological structure which was lined by pseudostratified columnar ciliated epithelium with mucous glands. Meanwhile, at 3 dpi, the tracheal mucosa showed focal deciliation and hyperemic blood capillaries with hyperplasia of the mucous gland. At 5 dpi, mucosal edema was detected that increased at 7 dpi, with focal aggregation of inflammatory cells. The severity of the tracheitis was increased at 10 dpi indicated by excessive deciliation and necrosis of mucous gland and tracheal mucosa that heavily infiltrated with mononuclear inflammatory cells with hyperemic blood vessels. Mucosal ulceration and metaplasia were noticed at 14 dpi.

The negative group exhibited normal lung lobules consisting of parabronchus, air, and blood capillaries. While 3 dpi examined parabronchi in the infected groups exhibited a proliferative response, characterized by hypertrophy of the smooth muscles and increased cellularity due to hyperplasia and metaplasia of the epithelium lining the parabronchi, atria, and infundibula. These changes were accompanied by infiltrating lymphohistiocytic cells at 5 dpi that increased within 7 dpi. Moreover, bronchitis with goblet cell hyperplasia was observed at 10 dpi with mononuclear cells infiltration that inclined at 14 dpi in addition to congestion of blood capillaries, inflammatory fluid exudation with lung consolidation.

Concerning the examined hepatic section, the negative control group displayed normal hepatic plates and portal triad. However, the challenge group showed vacuolar degeneration of hepatocytes at 3, 5 dpi. At 7 dpi, perivascular edema, congestion, and hyperplasia of bile duct were noted at portal area of infected birds. Prominent hepatocellular vacuolation and necrosis with mononuclear cell aggregation was recorded at 10 dpi and portal hepatitis was detected at 14 dpi.

Normal histological structure of renal tissue was detected in the control negative group. While experimentally infected group at 3 days showed congestion of blood capillaries with necrobiotic changes of the renal tubular epithelium as well at 5 dpi with hypercellularity of glomerular tuft. At 7 dpi, numerous glomeruli exhibited membranoproliferative glomerulopathy. At 10-14 dpi, the degree of nephritis was more intense.

The examined thymus of negative control group revealed normal histological structure of thymic tissues containing a plentiful population of lymphocytes. Mild depletion in the thymic lobules was observed at 3-7 dpi. At 10-14 dpi, severe vacuolation was found in the cortical zones indicating lymphocytic depletion and lymphocytolysis associated with thymic congestion and hemorrhagic.

Normal pancreatic tissue was observed in the control negative group. At 3 dpi, infected birds showed congestion and perivascular edema. Whereas, at 5 dpi, acinar epithelium suffered from vacuolar degeneration with sporadic apoptosis. At 7 dpi, the acinar cells were infiltrated with mononuclear cells and at 10 dpi, the acinar cells were severely depleted of zymogen granules with widespread apoptosis. The degeneration and apoptosis were extended to beta pancreatic islet at 14 dpi.

Negative control group had a normal intestinal morphology. On the other hand, an experimentally infected group showed mild infiltration of mononuclear inflammatory cells in the lamina propria at 3 dpi. The inflammatory reaction was elevated with hyperemic mucosa at 5-7dpi. Heterophilic infiltration with edema and cystic dilatation of crypt was noticed at 10 dpi. Severe enteritis was observed at 14 dpi, accompanied by necrosis of lamina epithelia.

Discussion

The LPAIV H9N2 virus is the most widespread avian influenza virus in the globe right now (Carnaccini, and Perez 2020). Since the 1990s, H9N2 virus has being endemic in poultry, with a fast increase in the number of countries affected by horizontal spread between poultry farms. in European countries, LPAI H9N2 is not recognized as a major animal health concern due to high sanitary standards, only sporadic cases are reported meanwhile it recoded to cause serious animal health problems and economic losses the Middle East, North Africa, and Asia (FAO, 2017; Nagy *et al.*, 2017). AI H9N2 is not a zoonotic virus by itself, but it can provide an internal gene to other zoonotic HA subtypes (H5 and H7), resulting in a new human pandemic (FAO, 2017). And since the infection with H9N2 virus is not notifiable so it considered a hidden threat to human and poultry industry (Naguib *et al.*, 2017; Bi *et al.*, 2022).

Hence, there is a great demand to follow up the circulating strain periodically. During our study the PM of the field infected chicks received to our laboratory showed caseous exudate in the bifurcation of the trachea, the same lesion previously observed with Bóna *et al.* (2023), where they find a fibrinous exudate at the bifurcation of the trachea due to AI H9N2. Experimental infection of one day old SPF chicks showed no
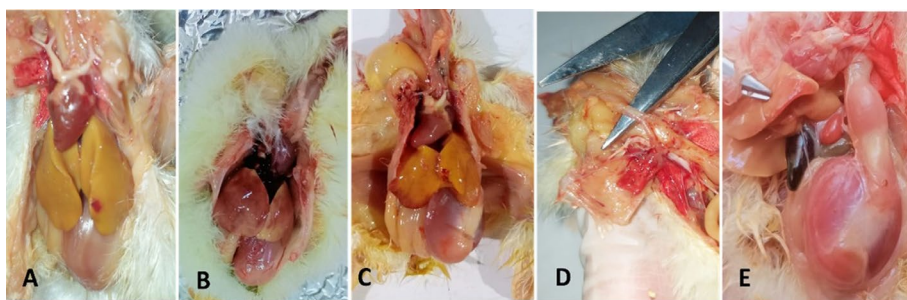
Fig. 3. PM of SPF chicks after AI H9N2 experimental infection shows: A, B & C: subcapsular hemorrhages in the liver; D: tracheitis & E: enlargement of spleen.

Fig. 4. PM of SPF chicks after AI H9N2 experimental infection shows: A: enteritis with unabsorbed yolk sac at 3 dpi; B: nephritis and nephrosis with distended ureter with urates, C: mild pneumonia and D: hemorrhages on the thymus gland.

mortality in all the experimental groups during the study period. From our observations, the main observed clinical signs in the experimentally infected chicks were depression and ruffled feathers only while during the different check points 3,5,7,10 and 14, dpi, there were different degrees of tracheitis, pneumonia, enteritis, nephritis, and nephrosis with distended ureters with ureates. On the same way Pourbakhsh *et al.* (2004); Hassan *et al.* (2020) recorded that the target organs for experimental H9N2 virus infection were the trachea and lungs, causing tracheitis and pneumonia. On the other hand, Slemons *et al.* (1990, 1991) did not report the involvement of the lungs when the infection was given through the intravenous route in chickens inoculated with waterfowl influenza viruses. Furthermore, several studies reported that H9N2 infected chickens produced prominent lesions in brain and kidneys in addition to respiratory

and gastrointestinal tracts in broiler chickens (Subtain *et al.*, 2011; Hassan *et al.*, 2017; Kye, *et al.*, 2021). Although there were no severe clinical signs appeared on the infected birds, histopathological examination revealed un expected results, where authors were suspected only respiratory (lung and trachea), renal and enteric virus tropism according to the previous records of (Subtain *et al.*, 2011; Begum *et al.*, 2023) also, because the LPAI virus replication is limited to respiratory and gastrointestinal tracts where the epithelial cells lining expressing trypsin (Swayne, 2007; Böttcher-Friebertshäuser *et al.*, 2013). Indeed, our results support those previously mentioned authors where trachea showed high score level at 10 and 14 dpi showing excessive deciliation and ulceration necrosis of mucous gland and tracheal mucosa that heavily infiltrated with mononuclear inflammatory cells with hyperemic blood vessels: 14 dpi, mucosal ulcer-
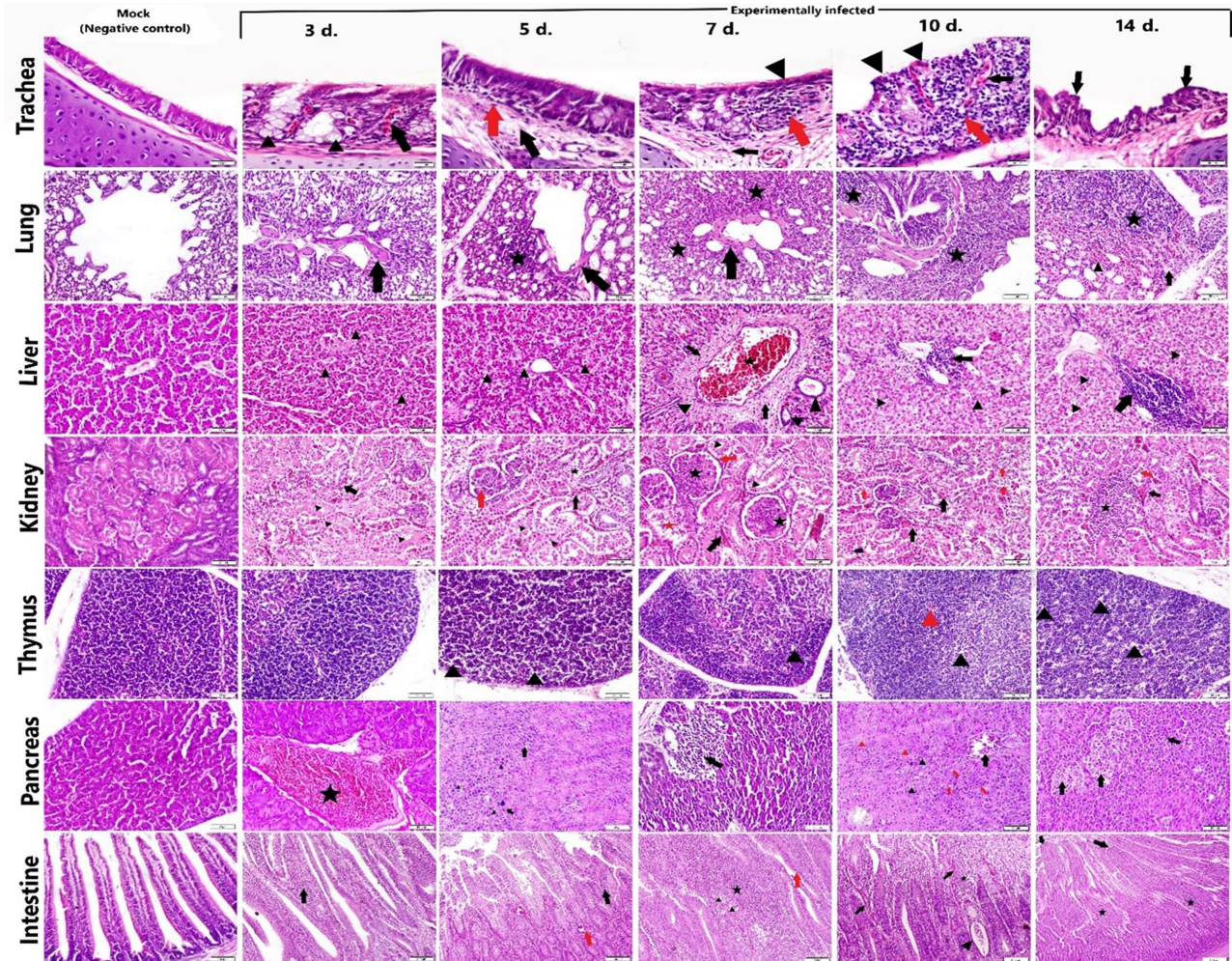
Fig. 5. Presenting the microscopic changes in different organs experimentally infected with H9N2 (H&E) Trachea: negative group showing normal tracheal histological structure ; infected group at 3 dpi, the tracheal mucosa showing hyperemic blood capillaries (black arrow) with hyperplasia of the mucous gland (black arrowhead) ; 5 dpi, tracheal mucosal showing focal aggregation of inflammatory cells (red arrow) with edema (black arrow) ; 7 dpi, deciliation (black arrowhead) of tracheal mucosal with focal aggregation of inflammatory cells (red arrow) and edema (black arrow) ;10 dpi excessive deciliation and ulceration (black arrowhead), necrosis of mucous gland and tracheal mucosa that heavily infiltrated with mononuclear inflammatory cells (red arrow) with hyperemic blood vessels (black arrow); 14 dpi, mucosal ulceration and metaplasia (black arrow). Lung: normal parabronchus in control negative group; infected group at 3 dpi, hypertrophy of the smooth of parabronchus (black arrow) ; 5&7 dpi, hypertrophy of the smooth of parabronchus (black arrow) with lymphohistiocytic cells aggregation (asterisk) ; 10 dpi, bronchitis with goblet cell hyperplasia and mononuclear cells infiltration (asterisk); 14 dpi, congestion of blood capillaries (black arrowhead), inflammatory fluid exudation (black arrow) and lymphohistiocytic cells aggregation (asterisk). Liver: negative group showing normal hepatic plates; infected group at 3&5 dpi showing hepatocellular vacuolation (black arrowhead) ; 7 dpi, congested blood vessels (asterisk), edema (black arrow) and hyperplasia of bile duct (black arrowhead); 10 &14 dpi, focal mononuclear cells aggregation (black arrow) with hepatocellular vacuolation and necrosis (black arrowhead).Kidney: negative group showing normal renal tubules and glomeruli; infected group at 3 dpi showing congestion of blood vessels (black arrow) with necrobiotic changes of the renal tubules(black arrowhead); 5 dpi, congestion of blood vessels (black arrow) with hypercellularity of glomerular tuft (red arrow) and cellular cast inside lumen of renal tubules (asterisk); 7 dpi showing thickening of Bowman's capsule (red arrow) , hypercellularity of glomerular tuft (black asterisk), congestion of blood vessels (black arrow), necrobiotic changes of the renal tubules (black arrowhead) with cellular cast inside lumen of renal tubules (red asterisk); 10 dpi showing congestion of blood vessels (black arrow) with necrobiotic changes of the renal tubules (red arrow); 14 dpi showing congestion of blood vessels (black arrow) with necrobiotic changes of the renal tubules (red arrow) and focal aggregation of mononuclear inflammatory cells (asterisk).Thymus: negative group showing normal histological structure of thymic tissues; infected group from 3 to 7 dpi showing depletion in the thymic lobules (black arrowhead); 10 & 14 dpi showing severe vacuolation at the thymic lobules (black arrowhead) with congestion (red arrowhead).Pancreas: negative group showing normal histological structure of pancreatic tissues; infected group at 3 days showing congestion of blood vessels (asterisk); 5 dpi, vacuolar degeneration (black arrowhead) and apoptosis (black arrow) of acinar epithelium; 7 dpi, infiltration with mononuclear cells (black arrow); 10 dpi showing congestion of blood vessels (black arrow), vacuolar degeneration (red arrow) and apoptotic spaces (black arrowhead) and necrosis (red arrowhead) of acinar epithelium; 14 dpi showing degeneration and apoptosis (black arrow) of acinar epithelium and cells of beta pancreatic islet. Intestine: negative group showing normal villi and crypt; infected group at 3&5 dpi showing infiltration of mononuclear inflammatory cells (black arrow), congestion of blood vessels (red arrow); 7 dpi ,goblet cells hyperplasia (red arrow), mononuclear inflammatory cells (asterisk) with inflammatory edema (black arrowhead); 10 dpi showing mononuclear inflammatory cells (asterisk),congestion of blood vessels (black arrow) with cystic dilatation of crypt (black arrowhead); 14 dpi showing thickening of intestinal mucosa with mononuclear inflammatory cells infiltration (asterisk) with necrosis of lining epithelium (black arrow).

ation, and metaplasia. Bronchitis with goblet cell hyperplasia congestion of blood capillaries inflammatory fluid exudation at 10 and 14 dpi, respectively with necrobiotic changes of the renal tubules with cellular cast inside lumen of renal tubules and focal aggregation of mononuclear inflammatory cells at 10 and 14 dpi. mononuclear inflammatory cells, congestion of blood vessels with cystic dilatation of crypt, thickening of intestinal mucosa with mononuclear inflammatory cells infiltration with necrosis of lining epithelium at 10 and 14 dpi.

During the work of Kye *et al*. (2021), the author emphasize on the need to study the pathogenesis of H9N2 in extrapulmonary tissues where they record the replication of H9N2 virus in brain, During our study the examined extrapulmonary tissues showed high pathological score where liver, pancreas and thymus were severely affected, and the severity of the lesion increased by the time period that reach high significant score (3.5, 3.2 and 3) respectively. Hyperplasia of bile duct at 10 and 14 dpi, focal mononuclear cells aggregation with hepatocellular vacuolation and necrosis. Vacuolar degeneration, apoptotic spaces and necrosis of acinar epithelium, and cells of beta pancreatic islet of pancreatic tissues at 10 and 14dpi. Depletion in the thymic lobules with severe vacuolation was observed on thymus gland at 7, 10 and 14 dpi. From all the above-mentioned results it is necessary to examine the circulating LPAI H9N2 annually from the molecular and the pathological aspects to determine whether the tissue of tropism is changed which may indicate mutation of the virus.

Conclusion

LPAI H9N2, is a serious immunosuppressive virus which plays a role in the exaggeration of the other co-infections. Periodical molecular monitoring of the circulating AIV with pathogenicity testing of these strains is critical for updating currently produced vaccines. The AI H9N2 virus in the current study was recovered from field cases with caseous plug at tracheal bifurcation instead of during the pathogenicity testing the virus induced only mild tracheitis. AI H9N2 alone, produce mild respiratory signs, with clear nephropathic changes without mortalities in SPF chicks. The virus tropism not restricted only to respiratory, renal, and gastrointestinal tract, but also to the liver, pancreas, and thymus. The authors recommend further full H9 sequence to perform cladogram to the currently tested viral strain with immunological evaluation in SPF chicks.

Acknowledgments

Conflict of interest

The authors declare that they have no conflict of interest.

References

Abd El-Hack, M.E., El-Saadony, M.T., Alqhtani, A.H., Swelum, A.A., Salem, H. M., Elbestawy, A. R., Noreldin, E.A., Babalghith, A.O., Khafage, A.F., Hassan, M.I., El-Tarabily, K.A., 2022. The relationship among avian influenza, gut microbiota and chicken immunity: An updated overview. Poult. Sci. 101, 102021. https://doi.org/10.1016/j.psj.2022.102021.

Amanollahi, R., Asasi, K., Abdi-Hachesoo, B., 2020. Effect of Newcastle disease and infectious bronchitis live vaccines on the immune system and production parameters of experimentally infected broiler chickens with H9N2 avian influenza. Comp. Immunol. Microbiol. Infect. Dis.71, 101492.

Bancroft, J.D., Layton, C., Suvarna, S.K., 2013. Bancroft's theory and practice of histological techniques. Churchill Livingstone Elsevier.

Begum, J.A., Hossain, I., Nooruzzaman, M., King, J., Chowdhury, E.H., Harder, T.C., Parvin, R., 2023. Experimental Pathogenicity of H9N2 Avian Influenza Viruses Harboring a Tri-Basic Hemagglutinin Cleavage Site in Sonali and Broiler Chickens. Viruses. 15, 461.

Bi, Y., Li, J., Shi, W., 2022. The time is now: a call to contain H9N2 avian influenza viruses. The Lancet Microbe. 3, e804-e805.

Bóna, M., Kiss, I., Dénes, L., Szilasi, A., Mándoki, M., 2023. Tissue Tropism of H9N2 Low-Pathogenic Avian Influenza Virus in Broiler Chickens by Immunohistochemistry. Animals 13, 1052.

Boroomand, Z., Jafari, R. A., Mayahi, M., 2018. Molecular detection and phylogenetic properties of isolated infectious bronchitis viruses from broilers in Ahvaz, southwest Iran, based on partial sequences of spike gene. In Veterinary Research Forum 9, 3, p. 279. Faculty of Veterinary Medicine, Urmia University, Urmia, Iran.

Böttcher-Friebertshäuser, E., Klenk, H.D., Garten, W., 2013. Activation of influenza viruses by proteases from host cells and bacteria in the human airway epithelium. Pathog. Dis. 69, 87-100.

Carnaccini, S., Perez, D.R., 2020. H9 influenza viruses: an emerging challenge. Cold Spring Harb. Perspect. Med. 10, a038588.

Chaharaein, B., Omar, A.R., Aini, I., Yusoff, K., Hassan, S.S., 2009. Detection of H5, H7 and H9 subtypes of avian influenza viruses by multiplex reverse transcription-polymerase chain reaction. Microbiol. Res. 164, 174-179.

Creelan, J.L., Graham, D.A., McCullough, S.J., 2002. Detection and differentiation of pathogenicity of avian paramyxovirus serotype 1 from field cases using one-step reverse transcriptase-polymerase chain reaction. Avian Pathol. 31, 493-499.

El-Zoghby, E.F., Arafa, A.S., Hassan, M.K., Aly, M.M., Selim, A., Kilany, W.H., Hafez, H.M., 2012. Isolation of H9N2 avian influenza virus from bobwhite quail (*Colinus virginianus*) in Egypt. Arch. Virol. 157, 1167-1172.

FAO, 2017. The State of Food and Agriculture (SOFA); FAO: Rome, Italy, 2017; ISBN 978-92-5-109873-8

Haghighat-Jahromi, M., Asasi, K., Nili, H., Dadras, H., Shooshtari, A.H., 2008. Coinfection of avian influenza virus (H9N2 subtype) with infectious bronchitis live vaccine. Arch. Virol. 153, 651-655.

Hassan, K.E., Ali, A., Shany, S.A., El-Kady, M.F., 2017. Experimental co-infection of infectious bronchitis and low pathogenic avian influenza H9N2 viruses in commercial broiler chickens. Res. Vet. Sci. 115, 356-362.

Hassan, K.E., King, J., El-Kady, M., Afifi, M., Abozeid, H.H., Pohlmann, A., Beer, M., Harder. T., 2020. Novel reassortant highly pathogenic avian influenza A (H5N2) virus in broiler chickens, Egypt. Emerg. Infect. Dis. 26, 129.

IVPI, 2022. The Intravenous Pathogenicity Index Test for Avian Influenza. [(accessed on 24 July 2022)]; Available online: https://science.vla.gov.uk/flu-lab-net/docs/protocol_IntravenousPathogenicity.pdf

Kishida, N., Sakoda, Y., Eto, M., Sunaga, Y., Kida, H., 2004. Co-infection of Staphylococcus aureus or Haemophilus paragallinarum exacerbates H9N2 influenza A virus infection in chickens. Arch. Virol. 149, 2095-2104.

Kiss, M.K., Kaszanyitzky, E., Chavez, Y., Johansson, K.E., 1997. Detection and identification of avian *Mycoplasmas* by polymerase chain reaction and restriction fragment length polymorphism assay. Vet. Micro. 58, 23–30

Kong, F., James, G., Gordon, S., Zelynski, A., Gilbert, G.L., 2001. Species-specific PCR for identification of common contaminant mollicutes in cell culture. Appl. Environ. Microbiol. 67, 3195-3200.

Kye, S.J., Park, M.J., Kim, N.Y., Lee, Y.N., Heo, G.B., Baek, Y.K., Shin, J.I., Lee, M.H., Lee, Y.J., 2021. Pathogenicity of H9N2 low pathogenic avian influenza viruses of different lineages isolated from live bird markets tested in three animal models: SPF chickens, Korean native chickens, and ducks. Poult. Sci. 100, 101318.

Mo, I.P., Brugh, M., Fletcher, O.J., Rowland, G.N., Swayne, D.E., 1997. Comparative pathology of chickens experimentally inoculated with avian influenza viruses of low and high pathogenicity. Avian Dis. 41, 125-136.

Monne, I., Hussein, H.A., Fusaro, A., Valastro, V., Hamoud, M.M., Khalefa, R.A., Dardir, S.N., Radwan, M.I., Capua, I., Cattoli, G., 2013. H9N2 influenza A virus circulates in H5N1 endemically infected poultry population in Egypt. Influenza and other Respiratory Viruses 7, 240-243.

Nagarajan, S., Rajukumar, K., Tosh, C., Ramaswamy, V., Purohit, K., Saxena, G., Behera, P., Pattnaik, B., Pradhan, H.K., Dubey, S.C., 2009. Isolation and pathotyping of H9N2 avian influenza viruses in Indian poultry. Vet. Microbiol. 13, 154-163.

Naguib, M.M., Ulrich, R., Kasbohm, E., Eng, C.L., Hoffmann, D., Grund, C., Beer, M., Harder, T.C., 2017. Natural reassortants of potentially zoonotic avian influenza viruses H5N1 and H9N2 from Egypt display distinct pathogenic phenotypes in experimentally infected chickens and ferrets. Journal of Virology 91, 10-1128.

Nagy, A., Mettenleiter, T.C., Abdelwhab, E.M., 2017. A brief summary of the epidemiology and genetic relatedness of avian influenza H9N2 virus in birds and mammals in the Middle East and North Africa. Epidemiol Infect. 145, 3320-3333.

OIE (Manual, Terrestrial), 2021. Chapter 3.3. 4. Avian influenza (including infection with high pathogenicity avian influenza viruses). Manual of Diagnostic Tests and Vaccines for Terrestrial Animals.

Peiris, M., Yuen, K.Y., Leung, C.W., Chan, K.H., Ip, P.L.S., Lai, R.W.M., Orr, W.K., Shortridge, K.F., 1999. Human infection with influenza H9N2. The Lancet 354, 916-917.

Perk, S., Golender, N., Banet-Noach, C., Shihmanter, E., Pokamunsky, S., Pirak, M., Tendler, Y., Lipkind, M., Panshin, A., 2009. Phylogenetic analysis of hemagglutinin, neuraminidase, and nucleoprotein genes of H9N2 avian influenza viruses isolated in Israel during the 2000–2005 epizootic. Comp. Immunol. Microbiol. Infect. Dis. 32, 221-238.

Pourbakhsh, S.A., Sohraby Haghdost, I., Hablolvarid, M.H., Gholami, M.R., 2004. Histopathological study of intratracheally inoculated A/Chicken/Iran/259/1998 (H9N2) influenza virus in Chicken. Arch. Razi Inst. 58, 51-62.

Pusch, E.A., Suarez, D.L., 2018. The multifaceted zoonotic risk of H9N2 avian influenza. Vet. Sci. 5, 82.

Reed, L.J., Muench, H., 1938. A simple method of estimating fifty per cent endpoints. Am. J. Epidemiol. 27, 493-497.

Rimi, N.A., Hassan, M.Z., Chowdhury, S., Rahman, M., Sultana, R., Biswas, P.K., Debnath, N.C., Islam, S.S., Ross, A.G., 2019. A decade of avian influenza in Bangladesh: Where are we now? Trop. Med. Infect. Dis. 4, 119.

Setta, A., Yehia, N., Shakak, A.O., Al-Quwaie, D.A., Al-Otaibi, A.M., El-Saadony, M.T., El-Tarabily, K.A., Salem, H.M., 2023. Molecular detection of highly pathogenic avian influenza H5N8 in commercial broiler chicken farms from 2019 to 2022. Poult. Sci. 102, 102639.

Slemons, R.D., Condobery, P.K., Swayne, D.E., 1991. Assessing pathogenicity potential of waterfowl-origin type A influenza viruses in chickens. Avian Dis. 35, 210-215.

Slemons, R.D., Locke, L.N., Sheerar, M.G., Duncan, R.M., Hinshaw, V.S., Easterday, B.C., 1990. Kidney lesions associated with mortality in chickens inoculated with waterfowl influenza viruses. Avian Dis. 34, 120-128.

Subtain, S.M., Chaudhry, Z.I., Anjum, A.A., Maqbool, A., Sadique, U., 2011. Study on pathogenesis of low pathogenic avian influenza virus H9 in broiler chickens. Pak. J. Zool. 43, 999-1008.

Swayne, D.E., 2007. Understanding the complex pathobiology of high pathogenicity avian influenza viruses in birds. Avian Dis. 51, 242-249.

WHO, 2020. World Health Organization. Influenza at the Human-Animal Interface Summary and Assessment, from 21 January to 28 February 2020. World Health Organization; Geneva, Switzerland: 2020. pp. 1–2.

WHO, 2019. World Health Organization. Influenza at the Human-Animal Interface Summary and Assessment, from 28 September 2019 to 25 November 2019. World Health Organization; Geneva, Switzerland: 2019. pp. 1–2.

Wu, R., Sui, Z.W., Zhang, H.B., Chen, Q.J., Liang, W.W., Yang, K.L., Xiong, Z.L., Liu, Z.W., Chen, Z., Xu, D.P., 2008. Characterization of a pathogenic H9N2 influenza A virus isolated from central China in 2007. Arch. Virol. 153, 1549-1555.

Xie, Z., Pang, Y. S., Liu, J., Deng, X., Tang, X., Sun, J., Khan, M.I., 2006. A multiplex RT-PCR for detection of type A influenza virus and differentiation of avian H5, H7, and H9 hemagglutinin subtypes. Mol. Cell. Probes. 20, 245-249.

Yehia, N., Salem, H.M., Mahmmod, Y., Said, D., Samir, M., Mawgod, S.A., Sorour, H.K., AbdelRahman, M.A., Selim, S., Saad, A.M., El-Saadony, M.T., 2023. Common viral and bacterial avian respiratory infections: an updated review. Poult. Sci. 102, 102553.